Fluctuation-induced interactions between dielectrics in general geometries

S. Pasquali and A. C. Maggs[a)]
Laboratoire de Physico-Chime Théorique, Gulliver CNRS-ESPCI 7083, 10 rue Vauquelin, 75231 Paris Cedex 05, France

(Received 24 January 2008; accepted 23 May 2008; published online 1 July 2008)

We study thermal Casimir and quantum nonretarded Lifshitz interactions between dielectrics in general geometries. We map the calculation of the classical partition function onto a determinant, which we discretize and evaluate with the help of Cholesky factorization. The quantum partition function is treated by path integral quantization of a set of interacting dipoles and reduces to a product of determinants. We compare the approximations of pairwise additivity and proximity force with our numerical methods. We propose a "factorization approximation" that gives rather good numerical results in the geometries that we study. © *2008 American Institute of Physics*. [DOI: 10.1063/1.2949508]

I. INTRODUCTION

Much is known about fluctuation-induced interactions between bodies.[1–3] At zero temperature, quantum fluctuations give rise to a multicenter generalization of London dispersion forces. For certain materials or for large length scales, thermal fluctuations can dominate, giving rise to the so-called thermal Casimir effect, which has as its origin the thermal excitation of polarization modes in dielectrics, giving rise to temperature dependent forces. In general, contributions come from an intrication of both thermal and quantum fluctuations. An alternative but equivalent vision comes from associating these forces with the energy and entropy of fluctuating electrodynamic fields. A number of sophisticated theoretical techniques have been applied to the calculation of this interaction but only the simplest of geometries are analytically tractable to exact solution, for instance, planar surfaces,[4] spheres, or cylinders.

More complicated physical situations are generally studied with perturbation theory, or in exceptional cases with nonperturbative methods adapted to individual geometries.[5] Such methods, which keep into account the totality of the interaction, are usually developed on the basis of Lifshitz theory for dielectrics. Analytic methods are typically based on an approximation around one of the few solvable problems. These range from the simple proximity force approximation to a semiclassical interactions approximation,[6] to the multipole expansion,[7] and to the more recent and sophisticated ray optics approximation.[8] The main problem with these methods is that they are limited when the system under study departs too far from the unperturbed system. Given the limitations of all analytic methods, which are in practice only capable of studying very regular geometries, numerical approaches have been developed. These methods have been limited both by storage space required and by long computational times, making it possible to study only two-dimensional systems or three-dimensional systems translationally invariant in one direction.[9,10] It is only very recently that more powerful methods have been developed based on the numerical calculation of the Maxwell stress tensor.[11] The numerical approach we present in this paper is complementary to this last method, but it is based on somewhat different theoretical grounds. We will explain in the discussion how the two methods compare in detail.

We note, as an aside, that the so-called "atomistic modeling" of materials, as performed with most molecular dynamics codes, with the aim of understanding micromechanical response, conformations of macromolecules or interfaces, often uses assumptions such as pairwise additivity of interactions[12] parametrized with phenomenological Lennard-Jones potentials. These methods neglect retardation, screening of the classical interaction by ions, and multibody effects. It is of clear interest to develop methods that will enable one to have a better quantitative understanding of such effects in both soft and hard condensed matter physics. More sophisticated (and even more costly) quantum simulation methods based on local density functionals exist but are known to miss long-ranged dispersion interactions completely.[13]

In this paper, we want to focus on important geometries that are clearly beyond perturbative study. One simple example is the case of a tip near a structured surface, where the curvature of the surface makes most approximation methods ineffective, unless the dielectric contrast is very weak.[14] This paper has as its principle aim the generalization of a recent paper,[15] which used direct diagonalization of a large matrix in order to calculate the free energy of fluctuating dielectrics in the classical (thermal Casimir) limit. The methods in Ref. 15 were rather limited, only very small three dimensional systems could be studied. Quantum effects were neglected entirely. In this paper, we use more sophisticated factorization techniques, which allow us to treat finer discretizations of physical systems. We will, in addition, show how to introduce quantum mechanics into our formalism and use it to study the full, nonretarded interaction between two dielectric bodies. In order to compare with our numerical method, we analyze the performance of two simple approximation methods: Pairwise additivity and the proximity force approxima-

[a)]Electronic mail: tony@turner.pct.espci.fr.

tion. We also introduce an approximation based on the factorization of the geometric and material properties that works surprisingly well for the geometries that we study.

We begin by formulating the theory of classical fluctuating dielectrics. In this, we prefer a formulation of the classical interaction in terms of the true microscopic fluctuating field, the polarization rather than the electric field and electric displacement. We then show how to efficiently factorize the resulting quadratic forms and apply our formalism to calculate the free energy of interaction between a tip and an indentation. We then generalize our microscopic energy functional in order to consider the quantum fluctuations of a dielectric and evaluate the nonretarded interaction between a tip and a structured surface.

II. CLASSICAL FLUCTUATING DIELECTRICS

We begin by evaluating the classical thermal interaction since most of the technical difficulties of discretization and factorization are already present before showing how to treat the quantum case. We start with the energy of a heterogeneous dielectric system[16] written in terms of the polarization density $\mathbf{P}$. We note that formulation in terms of the polarization field is also much more convenient for the generalization to scale dependent dielectric effects,[17] which are particularly important in water based systems.

The energy of a linear dielectric has two contributions,[16] firstly, a long-ranged Coulomb energy for the induced charged density $\rho_i = -\nabla \cdot \mathbf{P}$ and, secondly, a local contribution that depends on the local electric susceptibility $\chi_0(\mathbf{r})$,

$$U_p = \int \frac{\nabla \cdot \mathbf{P}(\mathbf{r}) \nabla \cdot \mathbf{P}(\mathbf{r}')}{8\pi|\mathbf{r}-\mathbf{r}'|} d^3r\, d^3r' + \int \frac{\mathbf{P}^2(\mathbf{r})}{2\chi_0(\mathbf{r})} d^3r. \quad (1)$$

We note that the dielectric constant $\epsilon(\mathbf{r}) = 1 + \chi_0(\mathbf{r})$, we use units where $\epsilon_0 = 1$. The partition function of the fluctuating dipoles

$$Z = \int \mathcal{D}\mathbf{P} \exp(-\beta U_p) \quad (2)$$

can be simplified by rewriting the Coulomb potential, $1/4\pi r$ as an integral over a potential ϕ. We then find the effective energy

$$U_{p,\phi} = \int \left(\frac{(\nabla\phi)^2}{2} - i\phi \nabla \cdot \mathbf{P} + \frac{\mathbf{P}^2(\mathbf{r})}{2\chi_0(\mathbf{r})} \right) d^3r. \quad (3)$$

One now performs the Gaussian integral over $\mathbf{P}$ to find the partition function expressed as an integral over ϕ.[18] To do this, it is useful to integrate by parts replacing $\phi \nabla \cdot \mathbf{P}$ with $-\mathbf{P} \cdot \nabla\phi$; boundary terms vanish in periodic systems or those in which fields decay at infinity.

In order to perform numerical calculations, we derive a discretized theory. We discretize by placing scalar quantities such as ϕ on $V = L^3$ nodes of a cubic lattice. We choose a length scale such that the lattice spacing is unity. The lattice spacing should be much larger than the atomic scale so that a formulation in terms of continuum dielectric properties is possible; the lattice should, however, be sufficiently fine to resolve features of physical interest, such as points or rough surfaces. Vector fields, such as $\nabla\phi$, are associated with the $3V$ links, ϵ and χ_0 are also associated with the links. We find

$$Z(\epsilon) = \prod_l \chi_{0,l}^{1/2} \int \mathcal{D}\phi \exp\left(-\beta \sum_l \frac{\epsilon_l}{2} (\partial_l \phi)^2 \right), \quad (4)$$

where l is a link; the discretization of the derivative ∂_l evaluates the difference between variables on the corresponding nodes. The integral in Eq. (4) is over all modes excluding the uniform mode, ϕ=const, which has an eigenvalue zero.[15] We write the quadratic form appearing in Eq. (4) as $\phi M \phi/2$ with a symmetric matrix M. The interesting, long-ranged part of the free energy of interaction comes from

$$\mathcal{F} = \frac{k_B T}{2} \log(\det'(M)), \quad (5)$$

where the determinant again excludes the zero eigenvalue. We will see that the advantage of working with a matrix of the form Eq. (4) rather than Eq. (1) is that the quadratic form Eq. (4) is sparse; a very large majority of its elements are zero, enabling the use of efficient evaluation strategies. While Eq. (1) is also Gaussian, its quadratic form is dense.

Some care has to be exercised to separate various contributions to the free energy Eq. (5). In most situations of interest, we want to find interfacial energies, which are subdominant compared with the bulk free energy of the full three dimensional system that we treat. The problem of separating bulk and surface contributions, in general, geometries is treated in a separate publication.[15] In the first physical example presented in this paper, the volume of each phase changes as the tip is moved farther from the indentation, and the surface free energy is obtained after subtracting the bulk free energy. In the second system, we analyze the volume of each phase is constant so that variations in the interfacial free energies can be found by simple subtraction, as the bulk contribution cancels out completely.

III. MATRIX FACTORIZATION

In the simplest geometries, such as multiple parallel plates, the determinant is evaluated analytically from the eigenvalue equations for sets of plane waves.[4] Since we wish to work in arbitrary geometries, we evaluate the determinant Eq. (5) using general matrix methods with periodic boundary conditions to minimize edge effects. Despite the fact that M is sparse and can be stored in memory, which is proportional to the volume $V = L^3$, standard (dense) matrix methods find the eigenvalues in a time that varies as $\tau_e \sim V^3$, using a storage $S \sim V^2$. Both these scalings turn out to be prohibitive and limit us to the study of systems no larger than linear dimension $L = 25$. We thus turn to methods that are adapted to large sparse matrices. For such matrices, it is preferable to evaluate the determinant without forming intermediate dense matrices, saving computer memory and accelerating calculations. We evaluate the determinant by firstly modifying the matrix in order to render it positive definite, so that we are not troubled by the zero eigenvalue. We do this by adding V to a *single* arbitrary diagonal element of the matrix; this can be shown to be equivalent to neglecting the zero mode of the determinant.[15] With the matrix, M now positive definite we

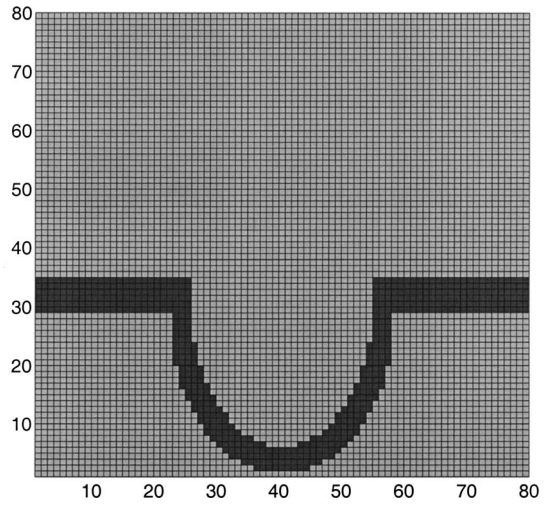

FIG. 1. Section of the tip-indentation system taken on a plane going through the center of the tip. The system is discretized to a lattice with $L=80$. The tip and the indentation are taken to be half ellipsoids with vertical semiaxes $a=18$ and horizontal semiaxes $b=15$ and $b=19$, respectively. In the figure, $l=6$.

write it as a product of Cholesky factors $M=R^TR$, where R is an upper triangular matrix. Because R is triangular, the determinant is given by the product of the diagonal elements. From the factor R, we find $\det M=(\det R)^2$.

This factorization has a number of remarkable properties that make it far more powerful than diagonalization. A good choice for the ordering that is used for evaluating the Cholesky factors renders the method particularly interesting: Nested dissection numbers the nodes in a nonconsecutive manner by recursively cutting a graph into equal pieces.[19] For this ordering of our matrix, the Cholesky factor (in three dimensions) can be generated with a storage of $S\sim V^{4/3}$, and with arithmetic effort $\tau_e\sim V^2$ (Ref. 20). We used the software package TAUCS (Ref. 21) to perform the Cholesky factoring. We find that a system of $V=64^3$ can be factored on a 3.2 GHz 64 bit Xeon workstation in approximately 300 s, using 3 Gbytes of memory.

IV. INTERACTIONS BETWEEN A TIP AND INDENTATION

We now consider the interactions between a tip and a surface indentation in a system in which the thermal contribution is dominant. Experimentally, this can occur in two physically distinct cases. Firstly, by use of matched material properties such as polymeric materials in contact with water; many such materials have similar optical properties to water so that the high frequency contributions to the Lifshitz energy cancel out. Secondly, the thermal contribution can dominate in nonmatched materials that are sufficiently separated; at room temperature quantum interactions die out for separations larger than $\hbar c/2k_BT\sim 5$ μm (Refs. 3 and 22).

We evaluated the free energy of interaction for a system composed of a three dimensional rounded tip close to an indentation in a surface discretized to a lattice of dimension $L=80^3$ (Fig. 1). We evaluated the free energies with two vertical displacements of $l=6$ and $l=20$. The physically interesting case for optically matched systems has a contrast ratio of approximately $r_\epsilon=\epsilon_1/\epsilon_2=50$ between the two media. However, in order to study the evolution of the interactions with contrast we worked with a minimum ratio of $r_\epsilon=1.05$ to a maximum of $r_\epsilon=100$.

In the absence of a general method to compute dispersion forces in arbitrary geometries, two approximations are commonly used. The first is the proximity force approximation according to which the interaction between surfaces of any geometry is found by assuming that the surfaces are locally flat. One then sums an effective, local free energy of the form

$$U(h,A)=\frac{A}{12\pi h^2} \tag{6}$$

over the surfaces, where h is the local distance between bodies and A is the Hamaker constant.

For the tip of Fig. 1, we compared results obtained via proximity force approximation with our numerical results for ratios of the dielectric constants varying from $r_\epsilon=1.05$ to $r_\epsilon=100$. In order to construct the proximity force approximation, for each lattice site of one surface we find the closest lattice site on the other surface and build a minimal distance map. We then use the generalization of Eq. (6) to periodic boundary conditions[15] to evaluate the interaction at each distance in the map and add all contributions to obtain the final free energy. The maps for the two chosen gaps are shown in Fig. 2. We find that the free energies computed with the proximity force approximation can deviate to up to 40% from the full numerical evaluation. In particular, the proximity force approximation performs worst for high dielectric contrast ($r_\epsilon=50$) and when the two surfaces are close together. This can be understood as being due to the sharp edges to the indentation with their associated high radius of curvature. Results for this system are shown in Fig. 3. When $l=20$, proximity force approximation performs better with deviations from the full evaluation of 8% for large contrast.

The second method, widely used in computer modeling, is an additivity assumption according to which the overall interaction is found by summing pairwise interactions of elementary components. A typical example of such approximation performs an integration of the long-ranged tail of Lennard-Jones $1/r^6$ potentials between infinitesimal constituents of the interacting macroscopic objects.[23] More generally, if one assumes a pairwise interaction between elements of a dielectric of the form $V(r)=\alpha v(r)$, where α characterizes the strength of the potential, then the long-ranged part of the interaction energy between two macroscopic bodies can be written as

$$U(\mathbf{R},\alpha)=\alpha G(\mathbf{R}), \tag{7}$$

where the coordinates $\mathbf{R}$ are the relative positions of the bodies and the function G encodes all the geometric information.

We notice that both Eqs. (6) and (7) display a factorization property (they are expressed as a product of material and of geometric terms) so that if we, for instance, consider the ratio

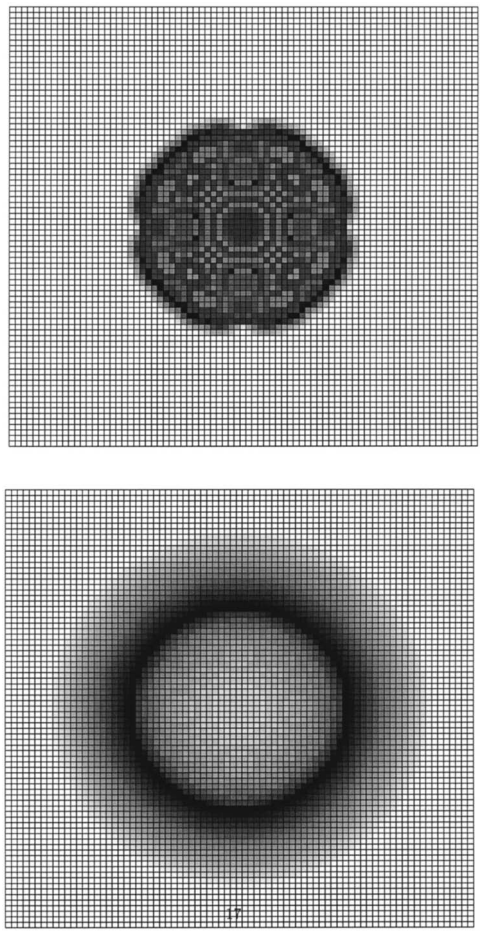

FIG. 2. Minimal distance map for $l=6$ (top) and $l=20$ (bottom). Black corresponds to the minimal distance, while white corresponds to the maximal distance. As the tip moves up, the geometry of the closest approach changes from a central disk to a ring from the rm of the indentation. Mesh corresponds to the discretization lattice.

$$\mathcal{R}_{12} = U(\mathbf{R}_1, \alpha)/U(\mathbf{R}_2, \alpha) \tag{8}$$

for two different geometries, we find a result independent of the material property. Since this factorization property is true in two very different limiting approximations it seems interesting to study the degree to which it remains valid over a wide range of dielectric contrasts in a geometry, which is far from planar.

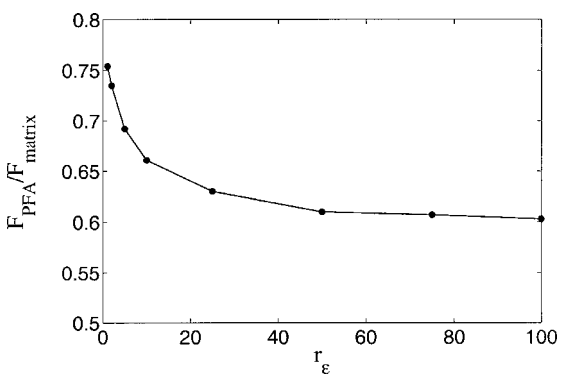

FIG. 3. Ratio between the free energies computed via proximity force approximation and our numerical results as a function of the dielectric contrast between the two materials for $l=6$.

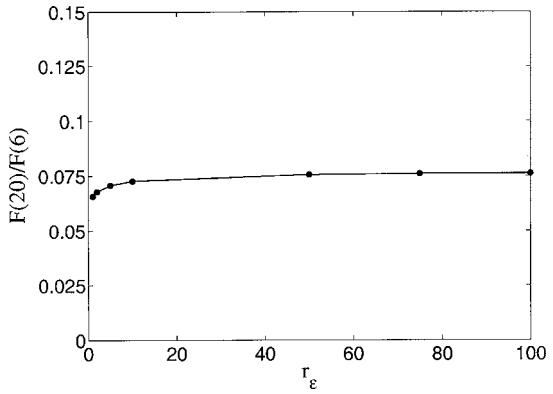

FIG. 4. Test of the factorization property [Eq. (8)]. The ratio of interaction energies for two separations of the tip-indentation system of Fig. 1 is plotted as a function of r_ϵ. The ratio varies by just 13% over the whole range of dielectric contrasts, despite the great variation in geometry displayed in Fig. 2.

Surprisingly, in Fig. 4, we find that the ratio of free energies computed at different distances exhibits only a moderate variation with the dielectric contrast. The robustness of this result has been tested by changing the system size and the accuracy of the tip/indentation discretization. Our study suggests a way of inferring free energy values at high dielectric contrast once the results at low contrast are known. It is sufficient to determine the interaction at low ϵ to obtain the whole set of measurements for the desired system. Our results show that for classical, thermal interaction, the factorization method we propose, works better than proximity force approximation when large surface deformations are present and for high dielectric contrasts, both instances where proximity force approximation performs poorly. This approach can be combined with analytic approximations that compute free energies for arbitrary geometries in a small dielectric contrast expansion.[14]

V. NONRETARDED QUANTUM INTERACTIONS

The quantum interaction between two materials is classified as nonretarded when the interaction is instantaneous, or retarded when one must take into account the finite propagation speed of electromagnetic radiation. In the first case, the decay of interactions between two atoms is $1/r^6$; in the second, the interaction falls as $1/r^7$. The characteristic crossover distance between these two forms is determined by the wavelength of typical spectral features that dominate dielectric response. This is often a feature in the ultraviolet, leading to a crossover length of tens of nanometers for most materials.

We now generalize our treatment of the interaction to the short distance, nonretarded regime. The systems for which this effect is dominant are limited to the nanoscale; however, we will show that this case is particularly simple to treat with the methods developed above. We leave the generalization to retarded interactions, which require the correct treatment of the propagating electromagnetic field, for a future publication.

A. Quantization

Since in the energy Eq. (1) the field **P** represents a microscopic polarization vector, we can study its dynamics by adding the kinetic energy

$$T = \rho \dot{\mathbf{P}}^2/2, \tag{9}$$

where ρ is a mass density that can, in principle, depend on the position.

The thermodynamics of a quantum system are particularly simple to treat with the method of path integral quantization.[24] The potential and kinetic energies are combined in an effective statistical weight for an ensemble of N identical replicas of the original system; these replicas are coupled in the time/temperature direction by harmonic springs. The exact quantum partition function is then generated in the limit of large N.

The effective action at each time slice, m is

$$U_m = \int d^3 r \frac{\rho(\mathbf{P}_m - \mathbf{P}_{m+1})^2}{2\hbar^2 \tau} + \tau U_p \tag{10}$$

with $\tau = \beta/N$. The harmonic coupling between the replicas comes from the presence of the terms in m and $m+1$ in Eq. (10) arising from the kinetic energy. We now perform a Fourier transform in the time/temperature direction and find that the energy can be written in a form, which is identical to Eq. (1) if we define a frequency dependent susceptibility

$$\frac{1}{\chi(\omega)} = \frac{1}{\chi_0} + \frac{\rho}{\hbar^2 \tau^2}(2 - 2\cos\omega)$$

with Fourier frequency $\omega = 2\pi n/N$.

We again perform the transformation from Eq. (1) to Eq. (3) by introducing an integral over the potential. After integrating over **P** the partition function of the quantum system is given by a product

$$Z = \prod_{n=0}^{N-1} Z(\epsilon(n)), \tag{11}$$

where in the $Z(\epsilon)$ of Eq. (4), the dielectric function is replaced by

$$\epsilon(n) = 1 + \frac{\chi_0}{1 + N^2(2 - 2\cos(2\pi n/N))/\hbar^2 \omega_0^2 \beta^2} \tag{12}$$

with $\omega_0 = 1/\sqrt{\chi_0 \rho}$. If we introduce the Matsubara frequencies $\omega_n = 2n\pi/\hbar\beta$, we find that for N large, Eq. (12) simplifies to the single pole approximation

$$\epsilon(n) = 1 + \frac{\chi_0}{1 + \omega_n^2/\omega_0^2} \tag{13}$$

often used[25] to fit the dielectric properties of material in calculations of the Hamaker constant. Passage to the limit Eq. (13) requires that

$$N^2 \gg (\hbar\omega_0\beta)^2 \epsilon(0) \tag{14}$$

in order that the high frequency limit $\epsilon(\omega) \to 1$ is correctly reproduced.

This path integral formulation gives the full, combined thermal and quantum contribution to the interaction potential. It does, however, become less efficient at low temperatures; at exactly zero temperature, the free energy should be evaluated by direct numerical quadrature over frequency.

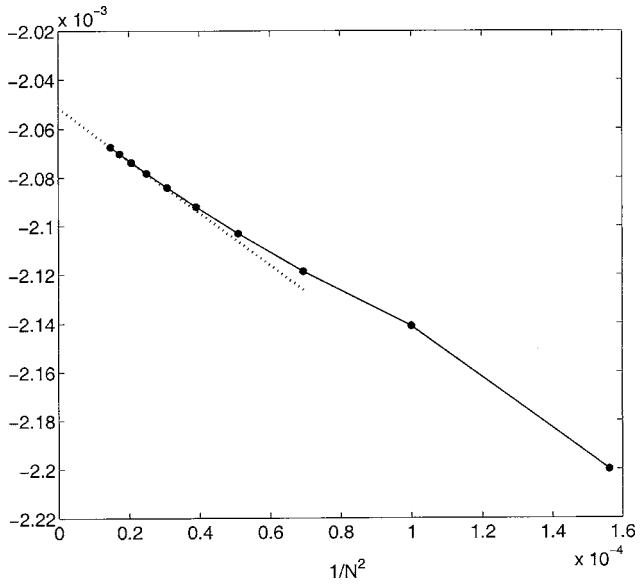

FIG. 5. Convergence of free energy differences with copy number N. We evaluated the free energy difference of two parallel plates separated by $l=2$ and $l=10$ for N varying from 80 to 260. The free energy is plotted as a function of N^{-2}. From values of N above 180 we extrapolate $F_\infty = 2.051 \times 10^{-3}$. $L=48$.

B. Implementation

Each contribution to Eq. (11) at frequency n requires the evaluation of a single matrix determinant identical in form to that evaluated in the classical interaction. We measured the absolute discretizion error by studying the free energy of interaction between two parallel slabs for different values of N. We followed the procedure in Ref. 15 using $\epsilon(0)=5$, $\hbar\omega_0\beta = 40$. If the largest contributions to the free energy comes from the ultraviolet range of the spectrum our choice of the parameters corresponds to a system near room temperature. Quantum effects then dominate the interaction but thermal effects are correctly included in the evaluation.

From Eq. (14), we require that $N \gg 90$. We performed evaluations of the free energy for $80 \leqslant N \leqslant 260$ (Fig. 5). Beyond $N=180$ the free energy can be fitted by the Richardson form $\mathcal{F} = \mathcal{F}_\infty + b/N^2$ (Ref. 26), where $\mathcal{F}_\infty$ and b are fitting parameters. Using values of N greater than 180 we estimate $\mathcal{F}_\infty$. We then evaluate the error generated for a specific value of N. We find an agreement that varies from 93% for $N=80$% to 99.0% for $N=260$. We adopted $N=240$ for the evaluation of the free energy landscape described below. For this value $\mathcal{F}_\infty/\mathcal{F}_{240} = 0.987$. Higher accuracy and faster convergence (in $1/N^4$) are possible if we work with two values of N and extrapolate to $\mathcal{F}_\infty$.

We then evaluated the free energy of a system composed of a sharp point over a surface with regular wells as a function of the horizontal position. Given that the typical small force microscopy tip sizes are of the order of 10–50 nm forces measured experimentally by this technique will generally fall into the crossover between the retarded and non-

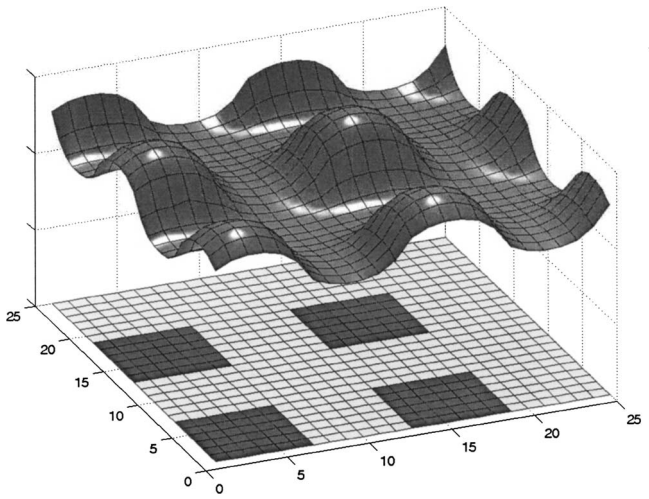

FIG. 6. Quantum free energy landscape for a system composed of a sharp, conical, tip near a surface with regular wells, side and depth $l=6$, separated by six lattice spaces in both x and y directions. Box size $L=48$. A portion of the system of dimensions 12×12 is scanned and the result reproduced periodically. Top surface: The free energy landscape at one lattice space above the top of the wells. Lower surface indicates the positions of the wells.

retarded regimes. However, there do exist extreme cases of tips of radii of 2 nm (super sharp silicon tips), where this case could be relevant, even if we are beginning to be close to the atomic scale where a continuum dielectric description is more difficult to justify.

We scanned a region of 12×12 lattice points, covering the area of one well and its surroundings. Results of the free energy landscape are shown in Fig. 6. The free energy of each point $\mathcal{F}(x,y)$ is evaluated for $N=240$, for which, due to the symmetry $\epsilon(n)=\epsilon(N-n)$, only $N/2+1=121$ determinants are needed. Firstly, the matrices $(12^2\times121\sim17\,500)$ were built using MATLAB and stored on disk. This took approximately 2 days on a single workstation. Then, the free energy evaluation was performed on a cluster of nine processors, and took approximately 2 days to complete, with the evaluation of the interaction at each position taking about 3 h. The energy landscape we obtained reflects the underlying well profile but with smoothed features.

VI. DISCUSSION

Quite fine and useful discretization of fluctuating dielectrics can be studied using methods based on Cholesky factorization of a sparse determinant. One can study the full multibody dispersion interaction at nanometric length scales, a scale suitable for the study of macromolecules and nanoparticles, in nontrivial three dimensional geometries. Conventional methods for interpreting such systems use extensive modeling with force fields that contain many simplifying assumptions, which can now be checked (in the near field regime) against explicit numerical results.

We now compare our approach with recent numerical work.[11] The authors work with the full discretized Maxwell equations that enable them to consider the full retarded interaction between bodies; they calculate the stress tensor rather than the free energy that we chose to evaluate. The method requires the calculation of the Green's functions, which are then integrated over a closed surface surrounding the body of interest. The authors propose several different methods of solving for the Green's functions, including fast multipole and multigrid methods, which they argue can solve the problem in with memory $S\sim V$ and time $\tau_e\sim V^{2-1/d}$. They work with modest system sizes of 20×40 in simplified $2+1$ dimensional geometries, suitable for studying grooved surfaces.

In practice, they used a conjugate method that requires a number of iterations, which increase with the systems size as $V^{1/d}$ (see Ref. 27) so that their actual implementation scales like our own as $\tau_e\sim V^2$. It could have been useful to compare real computing times, and not only theoretically derived asymptotic behaviors, but unfortunately the authors do not report these data. Any consideration of the choice of algorithm must take into account the prefactors in these laws; fast multipole methods have been abandoned in applications such as molecular dynamics due to the enormous prefactors in the (apparently favorable) asymptotic scaling.

For system sizes comparable to those used in this paper, one finds that the number of floating point operations needed to perform the Cholesky factorization is comparable to $N_{\text{flop}}=6.5V^2$ (see Ref. 28). Multigrid methods while being asymptotically fast can require hundreds of iterations in order to converge.[29] It thus seems possible that they perform less well than the methods of the present paper for moderate system sizes. It would be most interesting to study the crossover point in the efficiency of the various methods.

When we restrict ourselves to systems in $2+1$ dimensions, the Cholesky factorization we use also improves in performance. Storage requirement in this case is only $S\sim N\log(N)$, and computation time is $\tau_e\sim N^{4/3}$. The interaction of grooved surfaces is studied by Fourier transforming in the uniform direction before performing the factorization.[15] In such a system evaluation of the interaction of a system discretized to a lattice of dimensions 500^3 can be performed in 30 min on a 3.2 GHz 64 bit Xenon workstation.

The main physical problems that are still not possible to study with this method have length scales in the range of 20 nm–10 μm where the retarded interaction dominates. This requires a different discretization strategy based on the full Maxwell equations and will be considered in a future paper.[30]

ACKNOWLEDGMENTS

We wish to thank F. Nitti for many useful discussions. Work was financed in part by the Volkswagenstiftung.

[1] V. Parsegian and B. Ninham, Biophys. J. **10**, 664 (1970).
[2] B. Ninham and V. Parsegian, Biophys. J. **10**, 646 (1970).
[3] B. W. Ninham and J. Daicic, Phys. Rev. A **57**, 1870 (1998).
[4] B. W. Ninham and V. A. Parsegian, J. Chem. Phys. **53**, 3398 (1970).
[5] R. Buscher and T. Emig, Phys. Rev. A **69**, 062101 (2004).
[6] M. Schaden and L. Spruch, Phys. Rev. A **58**, 935 (1998).
[7] R. Balian and B. Duplantier, Ann. Phys. **112**, 165 (1978).
[8] R. L. Jaffe and A. Scardicchio, Phys. Rev. Lett. **92**, 070402 (2004).
[9] R. Buesher and T. Emig, Phys. Rev. Lett. **94**, 133901 (2005).
[10] H. Gies and K. Klingmüller, Phys. Rev. Lett. **96**, 220401 (2006).
[11] A. Rodriguez, M. Ibanescu, D. Iannuzzi, J. Joannopoulos, and S. Johnson, URL http://xxx.lanl.gov/pdf/0705.3661.

[12] W. Hofer, A. Foster, and A. Shluger, Rev. Mod. Phys. **75**, 1287 (2003).
[13] M. Ardhammar, P. Lincoln, and B. Nordn, Proc. Natl. Acad. Sci. U.S.A. **99**, 15313 (2002).
[14] R. Golestanian, Phys. Rev. Lett. **95**, 230601 (2005).
[15] S. Pasquali, F. Nitti, and A. Maggs, Phys. Rev. E **77**, 016705 (2008).
[16] R. A. Marcus, J. Chem. Phys. **24**, 966 (1956).
[17] A. C. Maggs and R. Everaers, Phys. Rev. Lett. **96**, 230603 (2006).
[18] M. Kardar and R. Golestanian, Rev. Mod. Phys. **71**, 1233 (1999).
[19] A. George, SIAM (Soc. Ind. Appl. Math.) J. Numer. Anal. **10**, 345 (1973).
[20] I. S. Duff, A. Erisman, and J. Reid, SIAM (Soc. Ind. Appl. Math.) J. Numer. Anal. **13**, 686 (1976).
[21] D. Irony, G. Shklarski, and S. Toledo, FGCS, Future Gener. Comput. Syst. **20**, 425 (2004).
[22] B. Cappella and G. Dietler, Surf. Sci. Rep. **34**, 1 (1999).
[23] C. Argento and R. French, J. Appl. Phys. **80**, 6081 (1996).
[24] D. M. Ceperley, Rev. Mod. Phys. **67**, 279 (1995).
[25] J. N. Israelachvili, *Intermolecular and Surface Forces* (Academic, New York, 1992).
[26] L. Brualla, K. Sakkos, J. Boronat, and J. Casulleras, J. Chem. Phys. **121**, 636 (2004).
[27] G. H. Golub and C. F. V. Loan, *Matrix Computations*, 2nd ed. (The Johns Hopkins University Press, Baltimore, 1989).
[28] P. R. Amestoy, I. S. Duff, J.-Y. L'Excellent, and X. S. Li, ACM Trans. Math. Softw. **27**, 388 (2001).
[29] A. J. Roberts, Aust N. Z. Ind. Appl. Math. J. **43**, E1 (2001).
[30] S. Pasquali, F. Nitti, and A. Maggs, "Numerical studies of Casimir Interactions," Phys. Rev. A (in press).